Weldability Characteristics of a New Corrosion- and Wear-Resistant Cobalt Alloy

Hot cracking sensitivity and weldment mechanical properties of a new cobalt-based alloy are investigated and characterized

BY S. J. MATTHEWS, P. CROOK, L. H. FLASCHE AND J. W. TACKETT

ABSTRACT. A study of the welding characteristics of a new cobalt-based alloy was performed. The Varestraint test was used to quantitatively investigate the fusion zone hot cracking resistance of three production heats. The average hot crack sensitivity of all three heats was found to be about the same as Alloy C-276, a highly alloyed nickel-based alloy with good resistance to hot cracking based on field experience. All three heats showed less hot cracking than either Alloy 25 (a heat-resistant, cobalt-based alloy) or Alloy 625 (another highly alloyed nickel-based alloy), which were also included in the test program.

For the purpose of gathering mechanical property data on weldments, plate materials were welded using gas tungsten arc welding (GTAW) and gas metal arc welding (GMAW). Weldment properties were characterized by high strength and limited ductility. Because of the limited ductility, transverse side bend and face/root bend test specimens were unable to undergo a 2T bend (bend radius twice the specimen thickness) without fracturing. When the bend radius was increased to a more generous radius (up to 4T), the frequency of bend failures decreased. A postweld solution heat treatment was found to improve bend ductility. A longitudinal face and root bend practice was eventually adopted for evaluation of laboratory weldments and is recommended for those fabricators interested in developing qualified welding procedures. A 3T longitudinal bend should produce acceptable results in the as-welded condition. Conclusions from this work are that fabricators should have no difficulty welding this cobalt-based alloy. Any significant cold forming or bending operations to be done on weldments after welding should be preceded by a 2050°F (1121°C) anneal.

S J. MATTHEWS, P. CROOK, L. H. FLASCHE and J. W. TACKETT are with Haynes International, Inc., Kokomo, Ind.

Paper presented at the 72nd Annual AWS Meeting, held April 14–19, 1991, in Detroit, Mich.

Introduction

For any new wrought alloy, it is essential that welding parameters be developed and weldment properties be evaluated. These data are critical to equipment and plant fabricators who are required to join and form such materials. The objective of this investigation was to generate preliminary welding information for a new cobalt-based material (Ref. 1) UNS R31233, commercially known as ULTIMET™[1] Alloy.

UNS R31233 is a solid-solution strengthened alloy. A typical wrought microstructure is shown in Fig. 1. The alloy is single-phase face centered cubic (FCC) in the solution annealed condition. The nominal composition of the alloy is presented in Table 1. Cobalt confers to the alloy's intrinsic resistance to wear and, as will be discussed, influences the mechanical properties of both the base metal and weldments, due to the allotropic phase transformation from FCC to a hexagonal close packed (HCP) crystal structure.

Chromium, molybdenum and tungsten serve dual functions in the alloy. They act as solid solution strengtheners and provide corrosion resistance. Chromium is of benefit in oxidizing acids, and molybdenum and tungsten are of benefit in nonoxidizing media, and all three elements are influential in resisting environments contaminated with chlorides. Nickel and iron serve to reduce the transformation temperature (*i.e.*, stabilize the more ductile, FCC phase), thus, enhancing hot and cold workability. The added ductility provided by these two elements also enhances resistance to stress corrosion cracking.

KEY WORDS

Cobalt Alloy
Weldability
Corrosion Resistance
Wear Resistance
Mechanical Properties
Solidification
Cracking
Varestraint Testing
Ductility
Bend Testing

Although present in small amounts, nitrogen and carbon are also key alloying elements. Control of these interstitials is critical to corrosion resistance (particularly localized attack) and wear properties (through their influence on deformation and fracture behavior). Silicon and manganese, as in most high-performance alloys, are added for fluidity and to tie up impurities, such as sulfur. The levels of carbon, silicon and manganese in the alloy were carefully selected so as to avoid the hot cracking susceptibility characteristic of other cobalt-chromium-molybdenum alloys, such as Alloy 21 (UNS R30021).

The material of this investigation was designed for service conditions involving simultaneous aqueous corrosion and wear (Ref. 2). In terms of chemical media, it possesses exceptional resistance to dilute sulfuric and hydrochloric acids, and all concentrations of nitric acid. It is particularly useful when acids are contaminated by oxidizing species. From a wear standpoint, the alloy excels under corrosive conditions involving cavitation erosion and slurry erosion.

Unlike the cast cobalt-based wear alloys, which contain carbide precipitates, UNS R31233 alloy exhibits considerable ductility in the solution annealed condi-

[1]*ULTIMET is a trademark of Haynes International, Inc.*

Table 1—Nominal Composition of UNS R31233 Alloy (wt-%)

Cobalt	Bal
Chromium	26
Nickel	9
Molybdenum	5
Iron	3
Tungsten	2
Manganese	0.8
Silicon	0.3
Nitrogen	0.08
Carbon	0.06

Table 2—Room and Elevated Temperature Tensile Properties of Solution Annealed Base Material

Temperature °F (°C)	0.2% Offset Yield Strength ksi (MPa)	Ultimate Strength ksi (MPa)	Elongation
70 (21)	79.3 (547)	147.8 (1019)	36.0
200 (93)	69.6 (480)	143.1 (987)	39.8
400 (204)	55.3 (381)	143.1 (987)	61.3
600 (316)	48.2 (332)	138.2 (953)	70.1
800 (427)	44.5 (307)	132.7 (915)	70.5
1000 (538)	38.4 (265)	125.0 (862)	69.8

Table 3—Chemical Composition of Production Heats (wt-%)

	Heat A	Heat B	Heat C
Co	Bal	Bal	Bal
Cr	24.89	26.20	25.83
Ni	8.96	8.85	9.06
Mo	4.69	5.12	4.94
W	1.81	2.49	2.07
Fe	3.06	3.15	3.11
Mn	0.72	0.69	0.66
Si	0.38	0.38	0.33
C	0.05	0.06	0.07
N	0.07	0.09	0.08

tion. Average tensile properties of annealed plate material in the temperature range 70°F (21°C) to 1000°F (538°C) are presented in Table 2. However, the material work hardens rapidly, as shown in Fig. 2 (a plot of hardness vs. cold work). The impact strength of the alloy at room temperature is about 130 ft-lb (176 joules).

In summarizing physical properties, this cobalt alloy is characterized by a high modulus of elasticity, high thermal conductivity and low electrical resistivity compared with the nickel-chromium-molybdenum corrosion alloys. The density of the alloy is 0.306 lb/in.^{3} (8.47 g/cm^3). The melting range is 2430° to 2470°F (1332° to 1354°C).

Experimental Procedure

Materials

Samples of plate from three different production heats were obtained for Varestraint weldability testing. Each heat was produced in a 15-ton electric arc furnace followed by argon-oxygen decarburization. The chemical analyses of the three heats are reported in Table 3. After electroslag remelting, ingots were forged and hot rolled to final size. Welding product was produced from Heat A by conventional forging, bar rolling and cold-wire-drawing manufacturing techniques.

The Varestraint test (Ref. 3) is well known in the literature as a means of characterizing hot-crack sensitivity. Full-size specimens, 12 X 2 X ¼ in. (300 X 50 X 6.3 mm), were prepared from each of the three production heats. In addition, identically sized specimens from three other alloys were obtained in order to compare relative hotcracking resistance. These were: Alloy 25 (UNS R30605), a wrought cobalt-based alloy also known as L-605; Alloy 625 (UNS N06625) and Alloy C-276 (UNS N10276), both of which are well-known nickel-based corrosion-resistant alloys.

Varestraint welding conditions were held constant for all alloys: 160 A, 15 V and 4½ in./min (114 mm/min) travel speed. Three test plates for each material were tested at each of three different augmented strain levels: 1.0, 1.33 and 2.0%. After testing, each specimen was examined for evidence of fusion zone cracking using a video microscope equipped with X-Y measuring stage and linear encoders. Cross hair positions of observed crack tips were collected on a personal computer, which then calculated total crack length for the specimen under observation. Average total crack length for each augmented strain level was then calculated and plotted in the usual manner.

Weldment Preparation and Testing

Welding was conducted in the laboratory to generate welded plate from which weldment mechanical properties could be measured and characterized. Both ½-in. (12.5-mm) thick and ¾-in. (19-mm) thick plates were welded using a single V-groove (70-deg included angle) and a ⅛-in. (3.2 mm) root opening. Plates were welded (no preheat) using both the manual gas tungsten arc (GTA) and the gas metal arc (GMA) welding processes. Maximum interpass temperature was

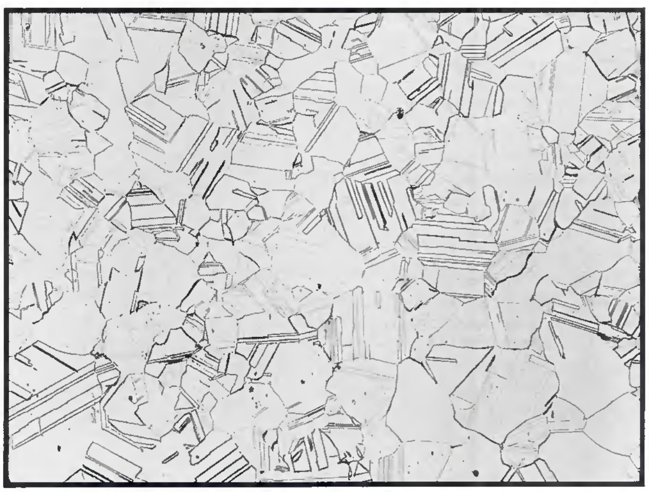

Fig. 1 — Optical photomicrograph of solution annealed alloy (UNS R31233). Magnification 300X. Hydrochloric acid and oxalic acid etch.

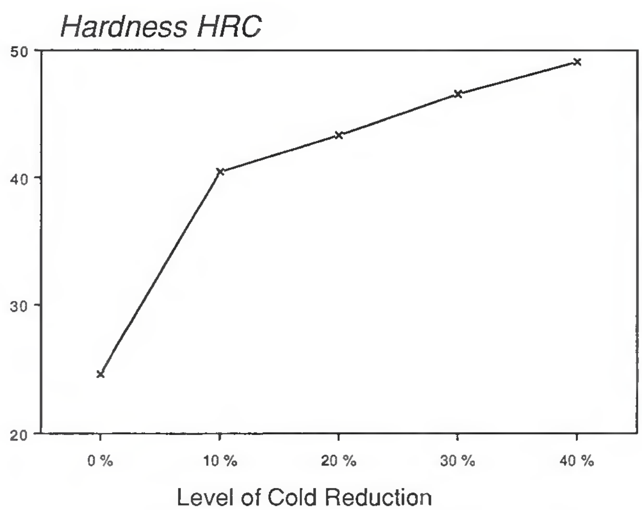

Fig. 2 — Base metal hardness as a function of percent cold reduction

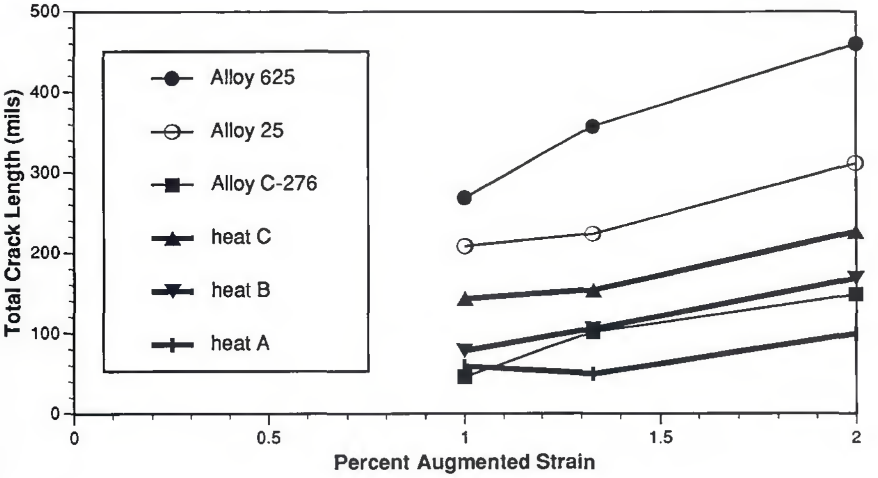

Fig. 3 — Varestraint test results for three production heats of UNS R31233. Each value plotted is an average of three tests.

Table 4—Welding Parameters

	GTAW	GMAW Short circuiting transfer	GMAW Spray transfer
Filler metal diameter in. (mm)	0.125 (3.2)	0.045 (1.1)	0.045 (1.1)
Amperage	160	150	250
Voltage	12	19	30
Wire feed speed in./min (m/min)	NA	200 (5.1)	335 (8.5)
Travel speed in./min (mm/min)	4 (100)	9 (229)	12 (305)
Shielding gas	Argon	Ar-He-CO_2 mixture[a]	Ar-He-CO_2 mixture[a]
Flow rate cfh (L/min)	30 (14.2)	35 (16)	35 (16)

(a) 10% He-0.25% CO_2-Bal. argon, patent allowed.

200°F (93°C). Other welding parameters used in the course of the data-gathering effort are documented in Table 4. GMA welding was performed in both the short circuiting transfer and the spray transfer mode, using a new shielding gas mixture developed by Haynes International. A key feature of the argon-helium-CO_2 mixture was the ability to weld in a variety of GMA transfer modes using a single shielding gas. The use of this mixture regardless of transfer mode resulted in excellent arc stability, weldability, bead profile and deposit cleanliness. After welding, plates were nondestructively examined by liquid penetrant and x-ray testing for welding defects. Plates were then sectioned by abrasive saw and machined into transverse tensile test specimens. Samples for guided bend testing were also prepared.

In addition to butt joint welded plate, several cruciform assemblies were fabricated using ½-in. (12.5-mm) plate. Multiple passes were then deposited into each of the four corner areas achieving enough buildup so as to allow the electrodischarge machining (EDM) of all-weld-metal test bars. These bars were subsequently machined into tensile test specimens. The successful welding of the cruciforms also served as a measure of the alloy's resistance to hot cracking under highly restrained conditions.

In addition to data gathering in the as-welded condition, duplicate sets of the specimen conditions were also subjected to a postweld solution heat treatment of 2050°F for 15 min and water quenched.

Metallurgical Investigation

Conventional metallography was used to characterize fusion zone microstructures generated during Varestraint testing. Crack tip regions were examined with a scanning electron microscope (SEM) equipped with an energy dispersive x-ray analyzer. The SEM was also employed to examine fracture surfaces created during bend testing. A transmission electron microscope (TEM) was also used to examine the weld metal substructure of a ¾-in.-thick plate GMA weldment. The TEM sample was prepared from a diamond saw slice removed from a weld metal sample obtained by EDM. The sample was carefully thinned by jet polishing (in a 30 vol-% solution of nitric acid in methanol). Thin-foil microscopy was performed at 100 kV.

Results and Discussion

Varestraint Testing

The Varestraint results are presented in Fig. 3, a plot of fusion zone hot cracking (total crack length) vs. percent augmented strain. For UNS R31233 alloy, the total crack length magnitude at each

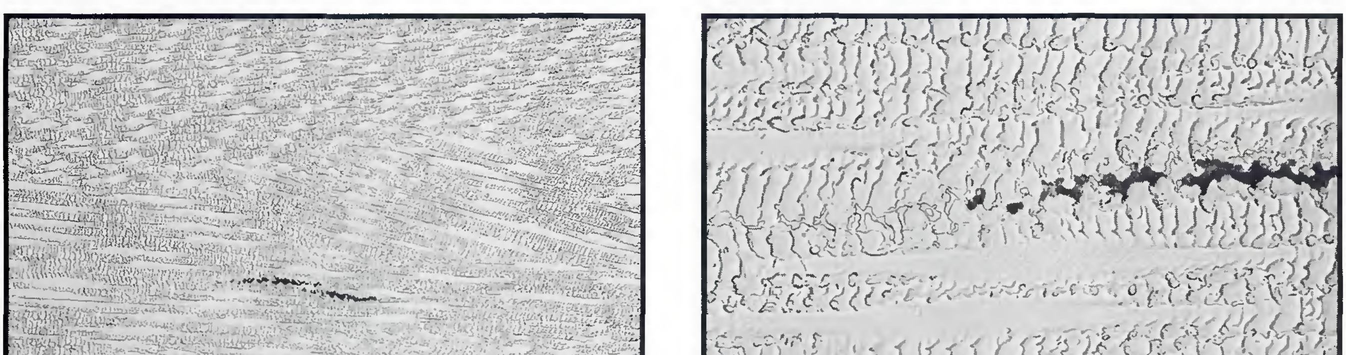

Fig. 4 — Photomicrographs of a fusion zone hot crack induced by the Varestraint test. HCl and oxalic etch. A — 100X; B — 500X, crack tip.

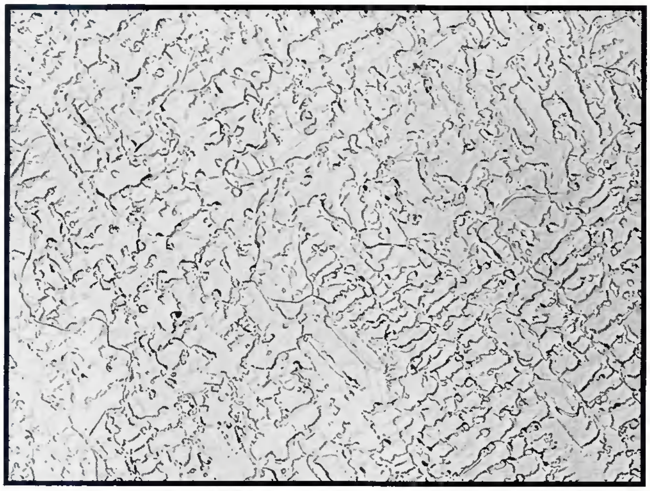

Fig. 5 — Typical weld metal microstructure (UNS R31233). GMAW deposit, short circuiting transfer. 500X magnification. HCl and oxalic etch.

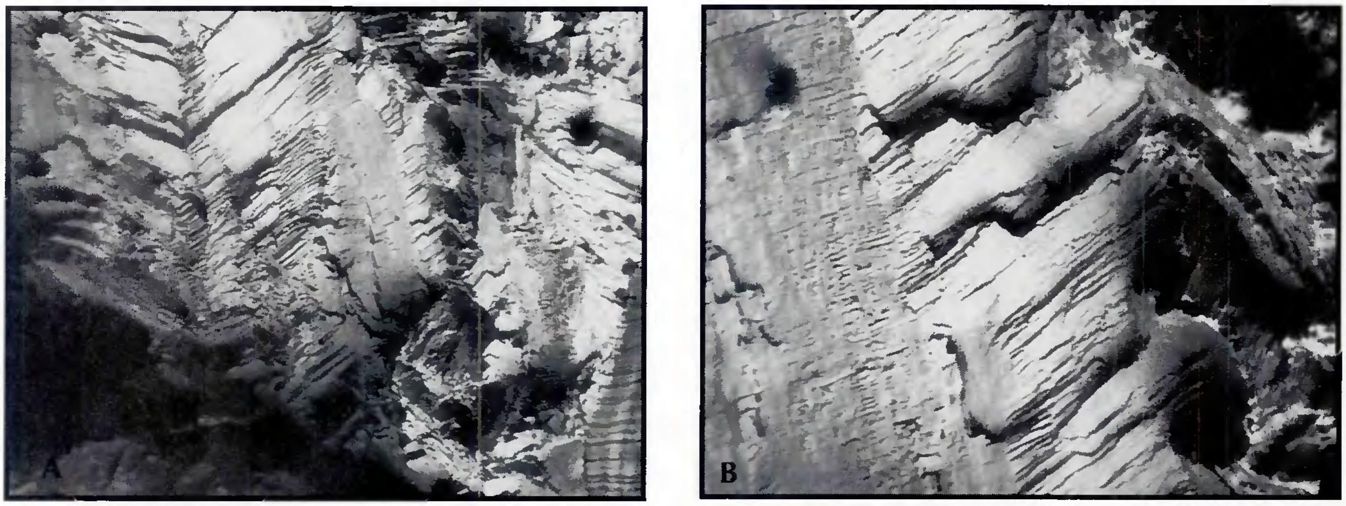

Fig. 6 — Scanning electron micrographs of a side bend fracture surface, 2½T bend radius, GTA welded ½-in. (12.5-mm) thick plate. A — 50X; B — 500X.

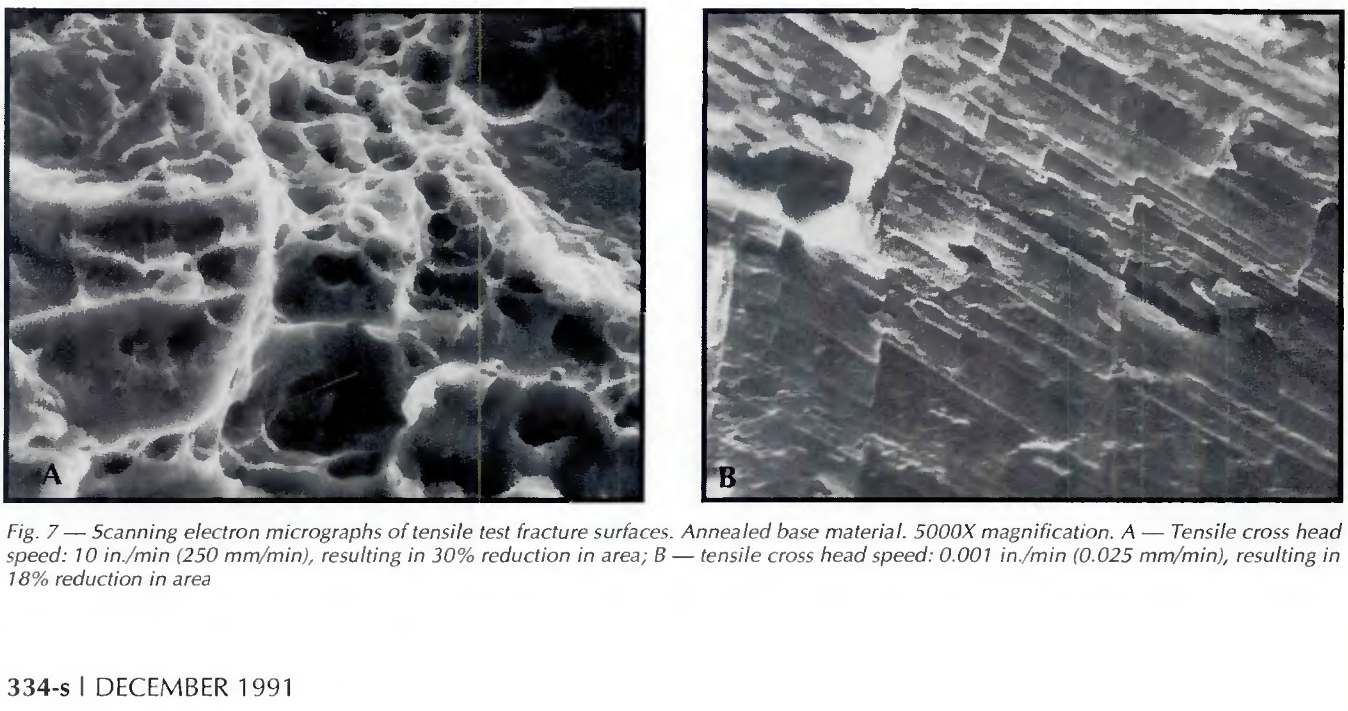

Fig. 7 — Scanning electron micrographs of tensile test fracture surfaces. Annealed base material. 5000X magnification. A — Tensile cross head speed: 10 in./min (250 mm/min), resulting in 30% reduction in area; B — tensile cross head speed: 0.001 in./min (0.025 mm/min), resulting in 18% reduction in area

strain level was found to be relatively low, indicating good resistance to fusion zone hot cracking. Also, the video microscope device used to collect the data was unable to detect any evidence of heat-affected zone hot cracking in any of the samples. As expected, some variation in heat-to-heat hot cracking sensitivity was measured, but these results are consistent with prior experience in Varestraint testing of multiple heats of solid solution strengthened nickel- and cobalt-based alloys. The average hot crack sensitivity of all three heats was found to be about the same as Alloy C-276, a highly alloyed corrosion-resistant nickel-based alloy with good resistance to hot cracking, based on field experience and other laboratory evaluations (Ref. 4). All three heats showed less hot cracking than either cobalt-based Alloy 25 (L-605) or Alloy 625. Figures 4A and 4B are photomicrographs of a fusion zone hot-crack induced by Varestraint testing. SEM microprobe analysis of the solidification segregation at the crack tip revealed enrichment in chromium and molybdenum and depletion in cobalt and nickel. A precise, quantitative characterization of the terminal solidification events was beyond the capability of the instrument.

Weldment Property Evaluation

The typical microstructure of deposited weld metal is shown in Fig. 5. Transverse tensile test results for ½-in.-thick (12.5-mm) and ¾-in.- thick (19.1-mm) welded plate are documented in Tables 5 and 6, respectively. All-weld-metal tensile results are reported in Table 7. Each value reported in Tables 5, 6 and 7 typically represents an average of two tests. A review of the data shows that in the as-welded condition, this alloy exhibits high strength: 85 to 98 ksi (584 to 675 MPa) yield strength and 123 to 136 ksi (851 to 938 MPa) ultimate tensile strength. A 2050°F postweld solution anneal served to reduce the yield strength to values in the vicinity of 71 ksi (490 MPa) and the ultimate tensile strength to about 121 ksi (835 MPa).

From Table 7 (all-weld-metal specimens), the ductility of the weld metal was measured to be between 10 to 18% elongation. As might be expected, the ability to successfully undergo a guided side bend test without fracturing is doubtful with a material of such intrinsic limited ductility. For example, it can be calculated that in order to conform to a 2T bend radius the outer fibers of the sample must have about 20% elongation; a 2½T bend radius requires 16.6% elongation, and a 3T bend requires about 12% elongation.

Table 5—Transverse Tensile Test Results Welded 0.5-in. (12.5-mm) Thick Plate

Welding Process	Condition	0.2% Offset Yield ksi (MPa)	Ultimate ksi (MPa)	Elongation %
Room Temperature				
GTAW	As Welded	88.7 (612)	126.8 (874)	10.7
GTAW	Solution Annealed	71.2 (491)	123.4 (851)	11.0
GMAW (spray transfer)	As Welded	92.7 (639)	133.4 (920)	10.6
GMAW	Solution Annealed	72.0 (496)	123.3 (850)	13.6
GMAW (short circuiting transfer)	As Welded	97.9 (675)	121.3 (836)	5.7
GMAW	Solution Annealed	71.6 (494)	120.7 (832)	13.1
500°F (260°C)				
GMAW (spray transfer)	As Welded	67.0 (462)	121.4 (837)	19.2
GMAW (short circuiting transfer)	As Welded	65.0 (448)	120.7 (832)	18.7
1000°F (538°C)				
GMAW (spray transfer)	As Welded	54.2 (374)	110.7 (763)	28.8
GMAW (short circuiting) transfer)	As Welded	52.8 (364)	114.4 (789)	28.4

Table 6—Tensile Test Results Welded 0.75-in (19.1-mm) Thick Plate

Welding Process	Condition	0.2% Offset Yield ksi (MPa)	Ultimate ksi (MPa)	Elongation %
Room Temperature				
GMAW (spray transfer)	As Welded	89.5 (617)	136.0 (938)	14.6
GMAW	Solution Annealed	75.4 (520)	130.2 (898)	17.6
GMAW (short circuiting transfer)	As Welded	85.8 (592)	123.4 (851)	10.2
GMAW	Solution Annealed	73.6 (507)	123.4 (851)	13.9
500°F (260°C)				
GMAW (spray transfer)	As Welded	64.4 (444)	120.7 (832)	23.3
GMAW (short circuiting transfer)	As Welded	62.3 (430)	116.6 (804)	19.8
1000°F (538°C)				
GMAW (spray transfer)	As Welded	49.5 (341)	112.7 (777)	32.1
GMAW (short circuiting transfer)	As Welded	44.6 (308)	97.7 (674)	25.8

Table 7.—Room Temperature All Weld Metal Tensile Test Results

Welding Process	Condition	0.2% Offset Yield ksi (MPa)	Ultimate ksi (MPa)	Elongation %
GTAW	As Welded	94.6 (652)	133.0 (917)	10.3
GTAW	Solution Annealed	70.6 (487)	120.5 (831)	12.9
GMAW (spray transfer)	As Welded	84.7 (584)	123.4 (851)	17.9
GMAW	Solution Annealed	67.3 (464)	119.9 (827)	21.5
GMAW (short circuiting transfer)	As Welded	88.6 (611)	131.5 (907)	17.3
GMAW	Solution Annealed	71.7 (494)	124.4 (858)	18.5

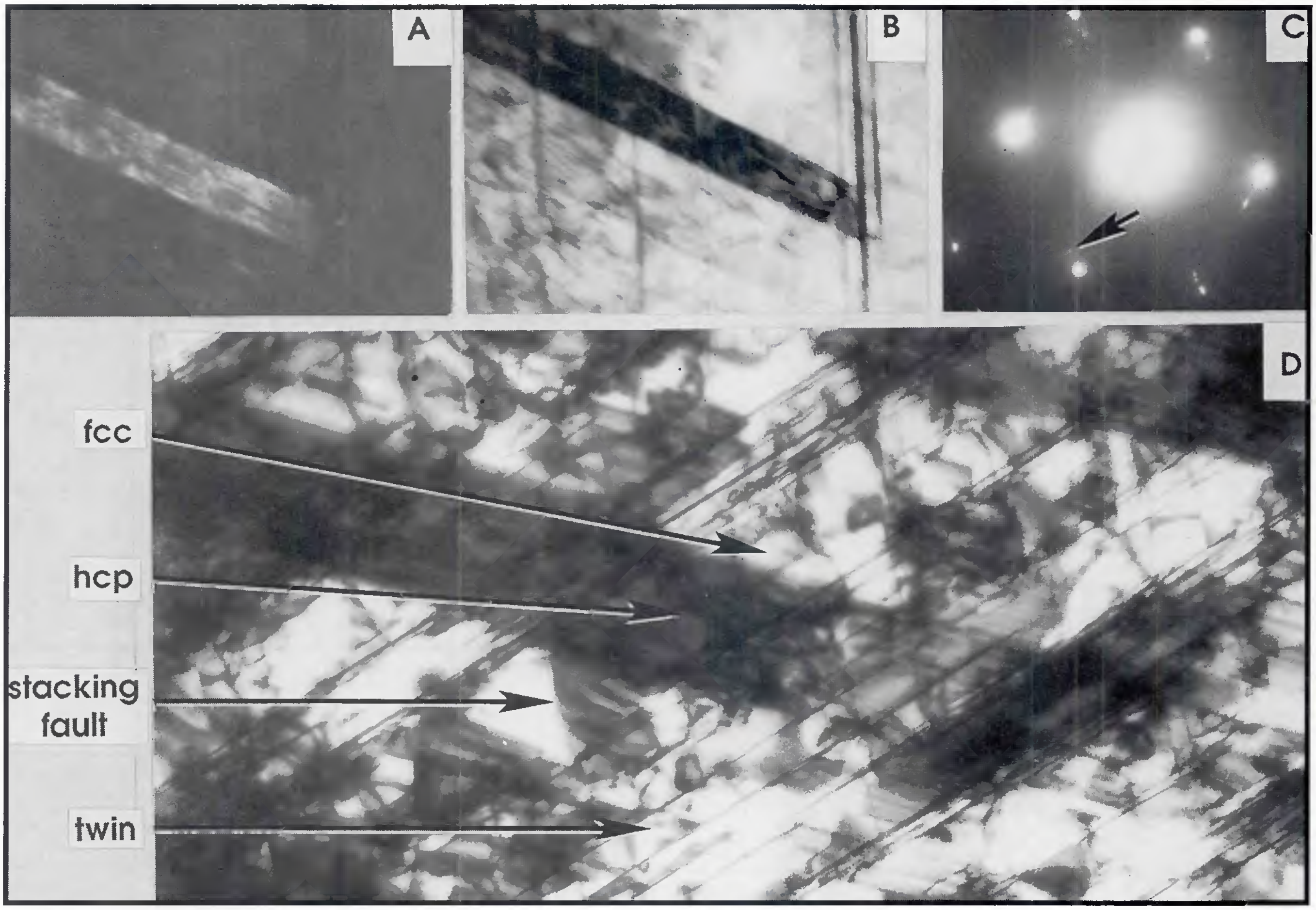

Fig. 8 — Transmission electron microscopy of UNS R31233 weld metal, 0.75-in. (19-mm) thick GMA welded plate (short circuiting transfer). A and B — Darkfield and bright-field micrographs (37,900 X) of HCP phase; C — corresponding [011] diffraction pattern. HCP streaking indicated by arrow. D — TEM micrograph (75,800X) showing FCC, HCP stacking faults and twins in as-deposited weld metal

During the early stages of weldment property evaluation, it was found that transverse side bend ductility test specimens and face/root bend ductility test specimens were unable to undergo a 2T bend without fracturing. When the bend radius was increased to 2½T, similar results occurred. When the bend radius was increased up to 4T, the frequency of side bend test fracturing decreased considerably, but results were inconsistent.

A longitudinal face and root bend practice was eventually adopted for evaluation of the laboratory weldments. In the course of welding procedure development, the use of longitudinal guided bend test specimens may be considered, especially when developing welding procedures for high-strength base metals. It was found that a 3T longitudinal bend specimen consistently produced acceptable results (*i.e.*, full 180-deg bends without fracturing).

Weld Metal Ductility Investigation

While the inability to pass a 2 or 2½T sidebend test was not surprising, a further investigation into the cause of limited weld metal ductility was deemed to be of interest. Figures 6A and 6B are SEM micrographs of a 2½T-sidebend fracture surface. The fracture appearance reveals considerable cleavage believed to be a result of stress-induced transformation from FCC to HCP crystal structure. This phenomenon is characteristic of cobalt-based alloys with low- stacking fault energy (Ref. 5).

It was reasonable to suspect that a stress induced transformation might be influenced by strain rate of the bend test. Guided bend tests are usually performed using a ram speed of 0.5 in./min (12.5 mm/min). A cursory investigation was conducted using nonwelded ½-in. (12.5-mm)-thick plate. Using the standard 0.5 in./min ram speed, the plate began to fracture after a 2T, 90-deg bend. A successful 2T, 90-deg bend, however, was made by bending at the maximum available ram speed of 10 in./min (250 mm/min). The effect of strain rate was further investigated by pulling nonwelded wrought tensile test specimens at the maximum cross head speed (10 in./min) and at the slowest available speed, 0.001 in./min (0.025 mm/min). The fracture results are shown in Fig. 7. Fracture characteristics of the fast strain rate showed evidence of ductile dimple rupture. The slow strain rate fracture revealed evidence of cleavage.

The strain rate of the mechanical property test, however, is not believed to be the only source of HCP transformation. During the course of bend test evaluations, it was found that a 2050°F postweld anneal, prior to testing, was able to dramatically improve the chances of undergoing a bend test without fracturing. It was assumed that this heat treatment completely restored a fully FCC crystal structure. This suggests that a stress-induced HCP transformation or at least a precursor to that transformation may occur after welding and not entirely during bend or tensile testing. It is reasonable to expect that this transformation on a local scale would be encouraged in weld metal microstructures where solidification segregation results in dendritic regions lean in FCC stability elements and enriched in HCP promoting elements.

Furthermore, it was found in a separate investigation aimed at generating tensile data for castings, that the ductility of cast alloy was higher than the ductility for weldments (*i.e.*, about 30% elongation vs. 17%). A plausible explanation for this is that weldments are characterized by considerable residual stress introduced, in part, by the restraint of the wrought base material. Residual stresses imposed upon the weld metal may be sufficient to at least partially induce a HCP transformation in the as-welded condition. Figure 8 documents high-magnification transmission electron microscopy performed on weld metal carefully removed from a ¾-in. (19.1-mm) thick weldment. The distinct appearance of HCP platelets and stacking faults (precursors to HCP platelets) supports the above hypothesis. The electron diffraction pattern also reveals characteristic "streaking," indicating the presence of HCP crystal structure within an FCC matrix.

Conclusions

1) The alloy of this investigation is a new cobalt-based material with good resistance to fusion zone hot cracking as measured by the Varestraint test and demonstrated by the ability to prepare highly restrained cruciform assemblies for all-weld-metal mechanical property characterization.

2) UNS R31233 plate can be readily fabricated using the GTA process and the GMA process in both the short circuiting and spray transfer modes.

3) Weldment mechanical properties are characterized by high strength and limited tensile ductility. Both conditions are a result of stress-induced, localized transformation from FCC to HCP.

4) For purposes of weld procedure development, a longitudinal face bend test specimen should be used as opposed to conventional transverse side bend or face bend testing. Properly deposited weld metal should take a 3T (bend radius equals three times specimen thickness) longitudinal bend without fracturing.

5) Fabricators should have no difficulty welding this alloy assuming sound welding practices are observed. If cold forming a weldment is necessary, where the bend radius is less than 4T, a solution anneal (2050°F/1120°C) followed by water quenching is recommended prior to forming.

Acknowledgments

The contributions of Haynes International welding laboratory technicians Messrs. M. A. Britton, J. L. Meyers and R. F. Polk are acknowledged. Also acknowledged is the electron microscopy work performed by B. E. Lewis.

References

1. Crook, P., Asphahani, A. I., and Matthews, S. J. 1991. Corrosion and wear resistant cobalt-base alloy. U.S. Patent 5,002,731.

2. Crook, P. 1990. A new corrosion and wear resistant high-strength cobalt alloy. *Cobalt News*, April.

3. Savage, W. F., and Lundin, C. D. 1965. The Varestraint test. *Welding Journal* 44 (10): 433-s to 442-s.

4. Cieslak, M. J., Headley, T. J., and Romig, A. D., Jr. 1986. The welding metallurgy of Hastelloy Alloys C-4, C-22, and C-276. Metallurgical Transactions A 17A (Nov):2035–2047.

5. Tawancy, H. M., Ishwar, V. R., and Lewis, B. E. 1986. On the fcc-hcp transformation in a cobalt-based superalloy (Haynes Alloy No. 25). *Journal of Materials Science Letters* 5:337-341.

WRC Bulletin 339
December 1988

Development of Tightness Test Procedures for Gaskets in Elevated Temperature Service
By A. Bazergui and L. Marchand

In this report, different elevated temperature gasket tightness test procedures are compared. A two-tier test approach, involving aging of the preloaded gasket in a kiln followed by a short duration tightness test was evaluated. The procedures were evaluated using spiral-wound gaskets with two different fillers: a mica-graphite filler and an asbestos filler.

Publication of this report was sponsored by the Subcommittee on Bolted Flanged Connections of the Pressure Vessel Research Committee of the Welding Research Council. The price of WRC Bulletin 339 is $16.00 per copy, plus $5.00 for postage and handling. Orders should be sent with payment to the Welding Research Council, 345 E. 47th St., Suite 1301, New York, NY 10017.

WRC Bulletin 344
June 1989

This Bulletin contains two reports covering three-dimensional finite element analysis of 45-deg lateral branch pipe models.

(1) Three-Dimensional Finite Element Analysis of PVRC 45-Degree Lateral Model 4 (d/D = 0.5, D/T = 40) under Out-of-Plane Moment Loading on Branch Pipes
By P. P. Raju

(2) Three-Dimensional Finite Element Analysis of 45-Degree Lateral Model 2 (d/D = 0.5, D/T = 10) under Out-of-Plane Moment Loading on the Branch Pipe
By P. P. Raju

Publication of these reports was sponsored by the Joint Task Group on Laterals of the Subcommittee on Piping, Pumps and Valves, and the Subcommittee on Reinforced Openings of the Pressure Vessel Research Committee of the Welding Research Council. The price of WRC Bulletin 344 is $16.00 per copy, plus $5.00 for U.S., or $8.00 for overseas, postage and handling. Orders should be sent with payment to the Welding Research Council, 345 E. 47th St., Room 1301, New York, NY 10017.

WRC Bulletin 346
August 1989

WFI/PVRC Moment Fatigue Tests on 4 × 3 ANSI B16.9 Tees

By G. E. Woods and E. C. Rodabaugh

The Markl-type fatigue test data presented in this report have been needed for a number of years to establish i-factors (SIFs) for forged tees with d/D ratios between 0.5 and 1.0 that conform to the ANSI B16.9 standard. These new data will provide improved design rules for both nuclear and industrial piping systems.

Publication of this report was sponsored by the Subcommittee on Piping Pumps and Valves of the Pressure Vessel Research Committee of the Welding Research Council. The price of WRC Bulletin 346 is $25.00 per copy, plus $5.00 for U.S. and $10.00 for overseas postage and handling. Orders should be sent with payment to the Welding Research Council, Room 1301, 345 E. 47th St., New York, NY 10017.